Phép đo tiết diện quá trình $pp \to W \to e\nu$ tại $\sqrt{s}$ = 14 TeV

Nguyễn Hải Dương* và nhóm hợp tác thực nghiệm CMS
*Bộ môn Vật Lý Hạt Nhân, Trường Đại Học Khoa Học Tự Nhiên Tp. HCM
227 Nguyễn Văn Cừ, Q. 5, Tp. HCM

Nhóm hợp tác thực nghiệm CMS dự định bắt đầu thu nhận các số liệu va chạm proton proton đầu tiên trong năm nay. Phép đo tiết diện tạo thành hạt *W* boson là một trong những phép đo đầu tiên sử dụng các số liệu này. Sản phẩm phân rã ở trạng thái cuối của các hạt *W* boson là các hạt lepton có năng lượng cao tạo ra những tín hiệu đặc trưng từ đầu dò CMS (Compact Muon Solenoid).Vì vậy, các sự kiện này là những đối tượng quan trọng để nghiên cứu sự xác định lepton và thực hiện các chuẩn hóa vật lý cho đầu dò CMS. Giả định lượng số liệu thu được từ sự va chạm proton proton tại $\sqrt{s}$ = 14 TeV là 10 pb^{-1}, chúng tôi nghiên cứu các phương pháp để đo tiết diện quá trình $pp \to W \to e\nu$.

Measurement of the Inclusive $W \to e\nu$ Cross Section in *pp* Collisions at $\sqrt{s}$ = 14 TeV

Duong NGUYEN (On behalf of the CMS Collaboration)
Department of Nuclear Physics, University of Natural Sciences
227 Nguyen Van Cu St., Dist. 5, Ho Chi Minh City, Vietnam

The CMS Collaboration plans to take its first data this year. The measurement of the W boson production cross section, which benchmarks the CMS (Compact Muon Solenoid) detector, will be one of the first physics measurements using these data. The high p_T leptons from leptonic decays of the W boson provide clean signals at CMS. Therefore, these events will be important candidates for understanding lepton identification and the physics commissioning of CMS. Assuming 10 pb^{-1} of pp collision data at $\sqrt{s}$ = 14 TeV, we investigate methods for a measurement of the inclusive W→eν production cross section.

1. Introduction

The W boson production cross section is an important Standard Model candle for the physics commissioning at CMS because of highly precise theoretical predictions and agreement between theory expectations and measured values [1, 2]. Moreover, the high transverse momentum (p_T) electron and the high transverse missing energy ($\not{E}_T$) from the $W \to e\nu$ decay provide distinct signatures for the CMS detector calibrations, especially the Trackers, the Hadronic (HCAL), and Electromagnetic (ECAL) Calorimeter subsystem calibrations. We follow the definition of the $W \to e\nu$ cross section as:

$$\sigma \times BR(W \to e\nu) = \frac{N_W^{pass} - N_W^{bkgr}}{A_W \times \varepsilon_W \times \int Ldt} \qquad (1)$$

N_W^{pass} and N_W^{bkgr} respectively correspond to the number of candidates selected from the data and the number of background events in the data. A_W is the acceptance defined as the fraction of decays satisfying the geometry constrains of the detector and the pre-selection kinematic constraints. ε_W is the selection efficiency of the W decays falling within the acceptance. $\int Ldt$ is the integrated luminosity. The data-driven methods for estimation of these quantities except the acceptance, which is calculated from Monte Carlo simulations, are discussed. The integrated luminosity measurement, which is expected to have at least 10% accuracy from an initial Van der Meer scan of the CMS beam spot size, is out of the scope of this article.

2. Event selection

First, the $W \to e\nu$ sample is selected by the CMS two-level trigger system, the Level-1 (L1) trigger and the High Level Trigger (HLT). The events are required to pass a trigger path which has a 12 GeV L1 trigger transverse energy (E_T) threshold on an electromagnetic shower deposited at a cluster of ECAL crystals and a 15 GeV (p_T) threshold on a reconstructed electron object at the HLT. In addition, the HLT electron is required to be isolated. Recent studies by CMS based on a trigger emulator have shown that the expected rate of the above trigger path is 17.1 ± 2.3 Hz at one of the start-up low luminosities (10^{32} cm^{-2} s^{-1}) and the overall efficiency (L1xHLT) for $W \to e\nu$ events is 62% [3].

In order to reject the background and extract the $W \to e\nu$ events from the above sample selected by the trigger, selection criteria are applied to the reconstructed electrons and missing transverse energy ($\not{E}_T$). The reconstructed electrons need to be formed from an electromagnetic shower in the ECAL within the fiducial region ($|\eta| < 1.5$ and $1.444 < |\eta| < 1.560$ excluded) and with $E_T \geq 20\,\text{GeV}$. Moreover, the electrons from the $W \to e\nu$ decays are isolated, thus we require a low track activity around the electron candidates which efficiently rejects electrons from the more frequent dijet events (QCD dijets) in *pp* collisions. On top of the above criteria, we apply electron identification cuts based on a detailed simulation study of the electron reconstruction and identification with some simplifications to obtain high efficiency and preserve discrimination power at the early data [4]. The $\not{E}_T$ is defined as the magnitude of the transverse vector sum over uncorrected energy deposits in the projective Calorimeter Towers [5]. Since the reliable $\not{E}_T$ correction may not be available in the early data, we don't apply any correction to the $\not{E}_T$, which has a mean value about 40 GeV for the $W \to e\nu$ decays, and set a cut at 20 GeV for the signal-background separation.

3. Selection efficiency

In order to measure the electron selection efficiency, we employ the so-called "Tag and Probe" method, which is successfully used by both Tevatron experiments and described in detail in another CMS note [6] . One tag electron is required to satisfy the tight electron identification criteria, thus it is considered as a good electron candidate. The other electron, called the probe electron, is used to estimate the efficiency of passing the considered cut. The total efficiency (ε_{total}) is factorized according to the subsequent reconstruction and selection steps of identifying an electron which are the triggering ($\varepsilon_{trigger}$), the preselection ($\varepsilon_{preselection}$), the isolation ($\varepsilon_{isolation}$), and the electron identification (ε_{elID}):

$$\varepsilon_{total} = \varepsilon_{trigger} \times \varepsilon_{preselection} \times \varepsilon_{isolation} \times \varepsilon_{elID} \tag{2}$$

In a detailed CMS study [6], $\varepsilon_{trigger}$, $\varepsilon_{preselection}$, $\varepsilon_{isolation}$, ε_{elID} have the values of 0.768 ± 0.005, 0.909 ± 0.003, 0.936 ± 0.003 and 0.997 ± 0.001, respectively. The efficiency of the $\not{E}_T$ cut can be estimated from the $\not{E}_T$ model of $W \to e\nu$ events which is described below.

4. Background estimation

Another important investigation is the background estimation. The largest contribution to the background comes from the QCD hadronic dijet events, where one jet results in an electron and the other jet is mismeasured, creating missing transverse energy. There are also electroweak (EWK) backgrounds, which consist most of the $Z/\gamma^* \to e^+e^-$ events with one electron misidentified (3% of signal), and the electron tau decays from W and Z bosons (2% of signal). The other processes ($W\gamma$, WW, WZ, ZZ, tW) have been found to be negligible. Compared to the QCD hadronic dijet background (QCD background), the EWK backgrounds are small and the cross sections of their processes can be reliably computed, thus they can be estimated with sufficient precision from simulation. Meanwhile, the QCD background arises from the strong interaction processes with large theoretical uncertainty in the cross sections. Therefore, it needs to be estimated by data-driven approaches. We use the so-called matrix method to fulfill that requirement. This method is based on the observation that the $\not{E}_T$ distribution of QCD dijet events passing the electron selection is fairly independent of the electron isolation criterion as shown in Figure 1. A control sample is derived by inverting the electron isolation cut of selection. As a consequence, that sample consists most of the QCD background events which in many cases fail the electron isolation cut. Beside the QCD

background events, the control sample contains negligible contamination from the electron-isolated $W \to e\nu$ signal events and the EWK background events.

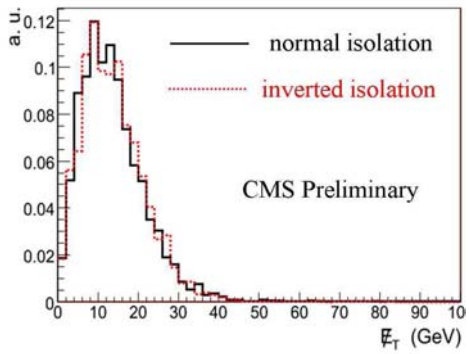

Figure 1: $\not{E}_T$ distributions of QCD dijet events which pass the electron selection with normal or inverted isolation requirements

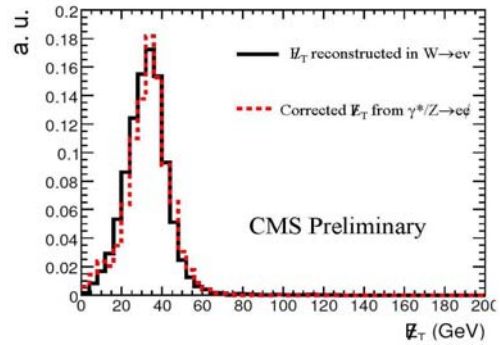

Figure 2: $\not{E}_T$ distributions reconstructed from $W \to e\nu$ events or estimated from $Z/\gamma^* \to e^+e^-$ events

Utilizing the above fact, from the control sample, one can derive a $\not{E}_T$ model for the QCD background events which mix with the $W \to e\nu$ signal events in the data selected by using the electron selections with a normal isolation cut. A factor, f_{QCD}, which is the ratio of the QCD events above and below the $\not{E}_T$ cut (20 GeV), is calculated from the $\not{E}_T$ model. Its value is $f_{QCD} = 0.2413 \pm 0.0019$ if the W and other EWK background in the control sample are properly subtracted. There is an increase of 7.8% if they are not subtracted from the control sample. Moreover, we measure a factor, f_Z, which is the same ratio as f_{QCD}, but estimated from a $W \to e\nu$ $\not{E}_T$ distribution model. This model is derived from the $Z/\gamma^* \to e^+e^-$ events by excluding calorimeter towers within a 0.1-radius cone in the $\eta - \phi$ plane around an electron. Figure 2 shows that the model and true $W \to e\nu$ $\not{E}_T$ distributions agree pretty well, thus f_Z has a value, $f_Z = 8.7 \pm 0.5$, which is close to the true value, $f_W = 8.13$, of the W $\not{E}_T$ distribution. The number of background and signal events above the $\not{E}_T$ cut in the data ($N_{>20}^{QCD}$ and $N_{>20}^{W}$ respectively) are the solutions of two equations:

$$N_{>20}^{QCD} = f_{QCD} N_{<20}^{QCD} = f_{QCD}\left(N_{<20} - N_{<20}^{EWK} - \frac{1}{f_Z} N_{>20}^{W} \right)$$
$$N_{>20}^{W} = N_{>20} - N_{>20}^{EWK} - N_{>20}^{QCD} \qquad (3)$$

$N_{<20}$ and $N_{>20}$ respectively correspond to the total number of events below and above the $\not{E}_T$ cut observed in the data. Their values are $N_{<20} = 136147$ and $N_{>20} = 94386$. The EWK background, estimated from simulation, contributes 6851 events to $N_{<20}$ ($N_{<20}^{EWK}$) and 3907 events to $N_{>20}$ ($N_{>20}^{EWK}$). Dividing $N_{>20}^{W}$ by the efficiency of the $\not{E}_T$ cut, $\varepsilon(\not{E}_T) = f_Z/(1+f_Z)$, one can get the total number of W events in the data:

$$N_{yield}^{W} = \frac{1+f_Z}{f_Z} N_{>20}^{W} = \frac{1+f_Z}{f_Z - f_{QCD}} \left(N_{>20} - N_{>20}^{EWK} - f_{QCD}\left(N_{<20} - N_{<20}^{EWK} \right) \right) \qquad (4)$$

Applying the formula results in 67954 ± 674 background-subtracted W events which is comparable with 67369 true W events in the signal/background cocktail. The $\not{E}_T$ distribution of the $W \to e\nu$ signal

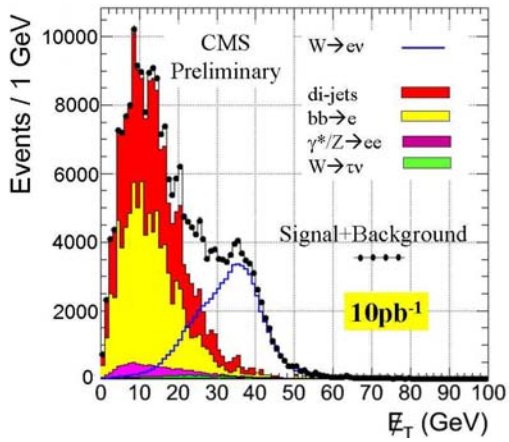

Figure 3: $\not{E}_T$ distributions of the $W \to e\nu$ signal events and the most important backgrounds after electron selection

and some sources of the backgrounds events in the data selected by the $W \to e\nu$ electron selection are shown in Figure 3. As can be seen, the most important background is contributed by the QCD light-flavor dijet and the heavy flavor *bb* events. These backgrounds are comparable to the signal, thus they need to be carefully controlled to reduce the systematic uncertainty.

5. Result

The results of the measurement are summarized in Table 1. $\varepsilon_{offline}$ is the product of $\varepsilon_{preselection}$, $\varepsilon_{isolation}$ and ε_{elID}. Note that Tag & Probe ε_{total} is the total electron selection efficiency which is substituted for ε_W into Equation 1. Thus N^W_{yield} is used to calculate the cross section.

N^W_{yield}	67954 ± 674
Tag and Probe $\varepsilon_{offline}$	84.8 ± 0.4 %
Tag and Probe $\varepsilon_{trigger}$	76.8 ± 0.5 %
Tag and Probe ε_{total}	65.1 ± 0.5 %
Acceptance, A_W	52.3 ± 0.2 %
Integrated luminosity, $\int Ldt$	10 pb^{-1}
$\sigma_W \times BR(W \to e\nu)$	19.97 ± 0.25 nb
Cross section used	19.78 nb

Table 1: Results for $W \to e\nu$ cross section measurement

The quoted uncertainties consist of only the statistical errors calculated from number of counted events. Although the systematic uncertainties are not considered in this analysis, they are known to be mainly dominated by the luminosity measurement uncertainty which is expected to be at least 10 %. As can be seen, there is an agreement within error between the measured cross section and the assumed next-to-leading-order cross section used to generate the $W \to e\nu$ sample. Detailed description of this analysis can be found at one of the references [7].

Acknowledgements

I'd like to thank Dr. Jeffrey Berryhill (Fermilab) and Prof. Greg Landsberg (Brown University) for their great guidances and helps. Many thanks to my colleagues, Aram Avetisyan and Dr. Chi-Nhan Nguyen, for their reviews and comments.

References

[1] D. Acosta et al. (CDF Collaboration), *Phys. Rev. Lett.* **94**, 091803 (2005)

[2] DØ Collaboration, *"Measurement of the Cross Section for W and Z Production to Electron Final States with the DØ Detector at* $\sqrt{s}$ *= 1.96 TeV"*, DØ Note **4403-CONF**, (2004)

[3] CMS Collaboration, "*CMS High Level Trigger*", CMS Note **2007/009**, (2007)

[4] S. Baffioni et al. (CMS Collaboration), *"Electron reconstruction in CMS"*, CMS Note **2006/040**, (2006)

[5] S. Esen et al. (CMS Collaboration), *"* $\not{E}_T$ *Performance in CMS"*, CMS AN **2007/041**, (2007)

[6] G. Daskalakis et al. (CMS Collaboration), *"Measuring Electron Efficiencies at CMS with Early Data"*, CMS AN **2007/019**, (2007)

[7] CMS Collaboration, *"Towards a Measurement of the Inclusive* $W \to e\nu$ *and* $\gamma^* / Z \to e^+e^-$ *Cross Sections in pp Collisions at* $\sqrt{s} = 14$ *TeV"*, CMS AN **2007/026**, (2007)

Địa chỉ liên lạc của tác giả:
Nguyễn Hải Dương
Bộ môn Vật Lý Hạt Nhân
Trường ĐH KHTN Tp. Hồ Chí Minh
227 Nguyễn Văn Cừ, Q. 5, Tp. HCM
Điện thoại: (08) 832-4468
E-mail: duong@fnal.gov